



Cite this: *RSC Adv.*, 2024, 14, 2705

# Coal gasification crude slag based complex flocculants by two-step acid leaching process: synthesis, flocculation and mechanisms

Haoqi Pan, Chenxu Sun, Tingting Shen, \* Jing Sun,\* Shaocang He, Tianpeng Li and Xuqian Lu

Coal gasification crude slag (CGCS) is the side-product of the coal gasification process, and its effective utilization has attracted great attention. A novel flocculant of poly-aluminum-ferric-acetate-chloride (PAFAC) was synthesized based on the recovery of CGCS by a two-step acid leaching process, namely HCl-acid leaching and HAc-acid leaching, which was optimized by an acid leaching liquor volume ratio of HCl to HAc of 3 : 2, polymerization pH of 3.5, and reaction temperature and time of 70 °C and 3.0 h, respectively. The performance of PAFAC was further evaluated by kaolin simulated wastewater, domestic sewage, river water, and aquaculture wastewater. The results revealed that PAFAC was feasible for the removal of turbidity, chemical oxygen demand (COD) and total phosphorus (TP). Moreover, PAFAC was characterized by X-ray Diffraction (XRD), Fourier transform infrared spectroscopy (FT-IR), X-ray fluorescence spectrometry (XRF) and scanning electron microscopy (SEM), which proved that PAFAC was a kind of amorphous polyionic composite. Additionally, the acid leaching kinetics and flocculation mechanisms were further investigated. It was found that the acid leaching process was followed by the unreacted shrinkage core model, and the flocculation process was dominated by charge neutralization, adsorption bridging and precipitation net trapping. The work is expected to develop a new method for the safe disposal of CGCS and provide a novel way for the preparation of Fe–Al composite flocculants, especially, offering a potential strategy for the promotion of the additional value of the coal chemical industry.

Received 24th October 2023  
Accepted 25th December 2023

DOI: 10.1039/d3ra07232k

rsc.li/rsc-advances

## 1. Introduction

Historically, coal has been China's primary source of energy due to the country's wealthy coal resources and lack of abundant oil and gas. It is foreseeable that the use of coal will continue to dominate China's energy structure for many years to come.<sup>1,2</sup> In 2021, China's raw coal production increased by 5.7% over the previous year, reaching a total of 4.13 billion tons. Furthermore, the country's coal consumption saw a rise of 4.6%.<sup>3</sup> Therefore, the efficient and clean utilization of coal is particularly important. Coal gasification is one of the core technologies for the efficient and clean utilization of coal,<sup>4</sup> and it is also the basis for the synthesis of many chemical products, such as the synthesis of methane,<sup>5</sup> methanol<sup>6</sup> and dimethyl ether.<sup>7</sup> The coal gasification process generates a solid waste, known as coal gasification slag including coal gasification crude slag (CGCS) and coal gasification fine slag (CGFS). It is reported that large quantities of coal gasification slag are discharged each year,<sup>8</sup> while its primary disposal methods are landfilling and stacking,<sup>9</sup> which

will lead to significant waste of land resources, and result in dust<sup>10</sup> and heavy metal<sup>11</sup> pollution, seriously harming the ecological environment and endangering human life. Thus, finding a practical solution for the disposal of coal gasification slag and its clean and efficient utilization is a challenge that ought to be addressed and developed in the future.

At present, the resource utilization of coal gasification slag is mainly focused on the following aspects: (1) production of building materials (*e.g.* wall material,<sup>12</sup> mixed cement,<sup>10</sup> aggregates,<sup>13</sup> pavement base materials<sup>14</sup>); (2) soil improvement (*e.g.* microbial diversity,<sup>15</sup> soil conditioner,<sup>16</sup> modification the structure of sand for planting<sup>17</sup>); (3) water remediation (*e.g.* zeolites,<sup>18,19</sup> adsorbent,<sup>20</sup> flocculants<sup>21</sup>); (4) other uses (*e.g.* plastic fillers,<sup>22</sup> cyclic mixing combustion,<sup>2</sup> hydrogen production,<sup>23</sup> CO<sub>2</sub> adsorption<sup>24</sup>).

As well known, flocculation has been widely used for the treatment of drinking water, domestic sewage and industrial wastewater,<sup>25,26</sup> and flocculants play a great role in the flocculation process. Compared to low molecular weight flocculants, polymer flocculants have the advantages of low dosage, fast settling, large flocs and insensitivity to pH in wastewater treatment, so polymer flocculants are currently more widely used in the water treatment process.<sup>25</sup> Polymer flocculants are mainly

School of Environmental Science and Engineering, Qilu University of Technology (Shandong Academy of Sciences), Jinan 250353, P. R. China. E-mail: shentingting@qlu.edu.cn; sunjing77@qlu.edu.cn



made from expensive chemicals, so the use of solid waste to prepare polymer flocculants is an economical and environmentally friendly path. For example, the application of red mud was challenging due to its complex composition, large specific surface area and high alkalinity.<sup>27</sup> Cheng *et al.*<sup>28</sup> prepared polymeric aluminum ferric chloride (PAFC) using acid leaching liquor of hydrochloric acid from red mud. Zhang *et al.*<sup>29</sup> mainly investigated the effect of the Al/Fe ratio of PAFC and alkalinity in the acid leaching liquor of fly ash, which resulted in 96.1% removal efficiency for SS and 91.5% for oil and grease. Recently, coal gasification slag was developed to prepare flocculants due to the abundant compositions of  $\text{Al}_2\text{O}_3$  and  $\text{Fe}_2\text{O}_3$ . He *et al.*<sup>21</sup> developed a one-step acid leaching process using HCl to extract the active components from CGCS and achieved a series of multi-ionic composite coagulants, which showed great coagulation efficiency for the treatment of kaolin simulated wastewater and domestic sewage. However, it was found that the leaching efficiency of CGCS was only about 65%, inhibiting the effective recovery of CGCS. Thus, finding a practical solution for the disposal of coal gasification slag and its clean and efficient utilization is a challenge that ought to be addressed and developed in the future.

It can be seen from the above research that the acid leaching method has a wide range of applications in the study of preparing flocculants from various minerals and solid wastes. However, the shortcomings of the one-step acid method lead to limited acid leaching efficiency, and the flocculation capacity cannot meet high application requirements. Additionally, the addition of chemical agents to modify the flocculant compound is not cost-effective. Therefore, some studies have explored the preparation of composite flocculants using a two-step acid leaching method involving HCl and  $\text{H}_2\text{SO}_4$ ,<sup>30</sup> but there are few studies on HCl and HAc. Moreover, HAc is a more environmentally friendly and cheaper acid compared to strong acids. In particular, HAc has a good effect on the leaching of iron, but its leaching ability for aluminum is weak.<sup>31</sup> This weakness allows it to play an advantage in adjusting the ratio of iron to aluminum on a macro level. It is expected to provide a potential way to prepare flocculants through the acid leaching process of solid waste recovery.

Therefore, in this work, a two-step acid leaching process, namely HCl-acid leaching and HAc-acid leaching, were initiated to extract effective ingredients from CGCS to overcome the shortcomings of the limited leaching efficiency. Firstly, the

processes were optimized by the acid concentration, acid leaching temperature, acid leaching time, and the liquid–solid ratio of acid to CGCS, respectively. Secondly, the two kinds of leaching liquor were mixed under optimal conditions, after a period of aging and drying, forming the flocculant of poly-aluminum-ferric-acetate-chloride (PAFAC). Thirdly, the performance of PAFAC was further evaluated by kaolin simulated wastewater, domestic sewage, river water, and aquaculture wastewater with the removal of turbidity, chemical oxygen demand (COD) and total phosphorus (TP). Moreover, PAFAC was characterized by X-ray Diffraction (XRD), Fourier transform infrared spectroscopy (FT-IR), X-ray fluorescence spectrometer (XRF) and scanning electron microscope (SEM). In addition, the acid leaching kinetics and flocculation mechanisms were further investigated. It is expected to propose a low-cost and high-value method of utilizing CGCS, and offer an environmentally friendly way for the preparation of inorganic polymer flocculants.

## 2. Materials and methods

### 2.1 Materials

Hydrochloric acid (HCl) was purchased from Yantai Yuandong Fine Chemicals Co., Ltd (China), sodium hydroxide (NaOH) was purchased from Foshan Xilong Chemical Co., Ltd (China), glacial acetic acid (HAc) and kaolin were both purchased from Sinopharm Chemical Reagent Co., Ltd (China). The CGCS used in this study was provided free of charge by Yankuang National Engineering Research Center of Coal Water Slurry Gasification and Coal Chemical Industry Co., Ltd, (Shandong, China). All reagents were analytically pure and did not require further treatment. All solutions were prepared with deionized water.

The domestic sewage and riverwater were provided by the reclaimed water station and Dacheng River located at Qilu University of Technology (Shandong, China), and the aquaculture wastewater was offered by a cow pasture (Shandong, China). The relevant water quality indexes are shown in Table 1.

### 2.2 Preparation of PAFAC

PAFAC was prepared according to the following three steps: HCl-acid leaching process, HAc-acid leaching process and the associative polymerization, which was carried out by a mixture of the leaching liquor of HCl and HAc acid leaching process. The entire process is shown in Fig. 1.

Table 1 Relevant water quality indexes used in this work

Items	Pollutant concentration			
	Turbidity (NTU)	COD (mg L <sup>-1</sup> )	NH <sub>3</sub> -N (mg L <sup>-1</sup> )	TP (mg L <sup>-1</sup> )
Kaolin wastewater	958.40	n.d. <sup>a</sup>	n.d.	n.d.
Domestic sewage	118.52	481.20	87.72	2.85
River water	120.20	280.60	87.61	3.10
Aquaculture wastewater	4220	7280	165.2	77.76

<sup>a</sup> n.d. indicates not detected.



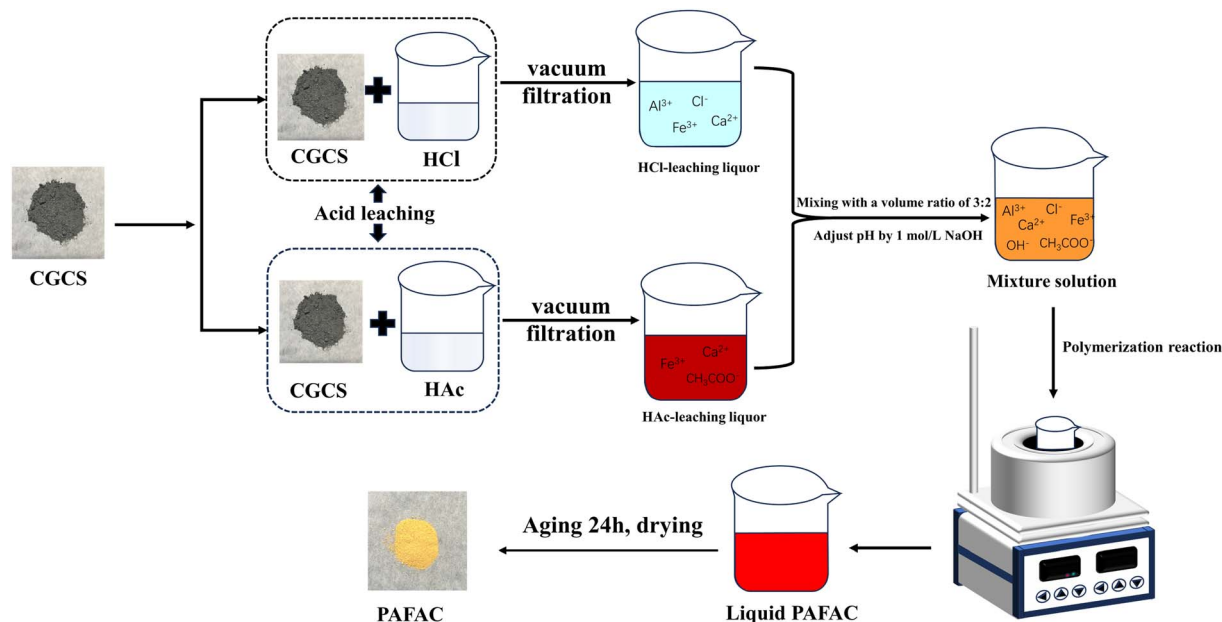


Fig. 1 The process of PAFAC preparation from CGCS.

**2.2.1 HCl-acid leaching process.** In a 500 mL beaker, CGCS and HCl solution of a certain concentration (1.0, 2.0, 3.0, 4.0, 5.0 mol L<sup>-1</sup>) were added at a certain liquid–solid ratio (mL : g) (5 : 1, 10 : 1, 15 : 1, 20 : 1, 25 : 1). The beaker was sealed with parafilm, put in a thermostat water bath (DF-101S, Gongyi City Yuhua Instrument Co., Ltd, China), and stirred at a set temperature (20, 30, 40, 50, 60 °C) for a period of time (0.5, 1.0, 1.5, 2.0, 2.5 h). It was then filtered and separated by a vacuum filter (SHK-III, Zhengzhou Ketai Laboratory Equipment Co., Ltd, China), and the HCl-leaching liquor was obtained for the preparation of PAFAC. The filtrate residue was repeatedly rinsed with deionized water and then dried and weighed for calculating the leaching rate.

**2.2.2 HAc-acid leaching process.** In a 500 mL beaker, CGCS and HAc solution of a certain concentration (2.0, 3.0, 4.0, 5.0, 6.0 mol L<sup>-1</sup>) were added at a certain liquid–solid ratio (mL : g) (5 : 1, 10 : 1, 15 : 1, 20 : 1, 25 : 1), and the beaker was sealed with parafilm, put in a thermostat water bath, and stirred at a set temperature (20, 30, 40, 50, 60 °C) for a period of time (0.5, 1.0, 1.5, 2.0, 2.5 h). Afterward, it was filtered and separated by a vacuum filter, and the HAc-leaching liquor was obtained for the preparation of PAFAC. The filtrate residue was repeatedly rinsed with deionized water then dried and weighed, and was used for calculating the leaching rate.

**2.2.3 Associative polymerization.** The HCl-leaching liquor and the HAc-leaching liquor were mixed according to a certain volume ratio (5 : 1, 3 : 1, 2 : 1, 3 : 2, 1 : 1, 2 : 3), and the pH was adjusted to a certain value (2.0, 2.5, 3.0, 3.5, 4.0, 4.5, 5.0) with NaOH solution. Then heated and stirred at a set temperature (50, 60, 70, 80, 90 °C) for a period of time (1.0, 2.0, 3.0, 4.0, 5.0 h). After the reaction was completed, the mixture solution was aged for 24 h, then dried in a constant temperature drying oven to synthesize PAFAC, which was ground into powder for use.

## 2.3 Performance investigations on PAFAC

**2.3.1 Flocculation process.** Flocculation experiments were conducted on a flocculation mixer (MY3000-6, Wuhan Meiyu Instrument Co., Ltd, China). 200 mL of simulated wastewater or actual wastewater was taken into a beaker, the flocculant was added and then stirred. The flocculation process was set as follows: first, rapid stirring at 250 rpm for 30 s, then slow stirring at 60 rpm for 20 min, and standing for 15 min. The treatment efficiency of turbidity, COD, NH<sub>3</sub>-N and TP were used to evaluate the performance of PAFAC. The supernatant was taken below 2 cm from the surface of the water and detected for turbidity with a turbidimeter (WGZ-3, Shanghai Xinrui Instruments & Meters Co., Ltd). NH<sub>3</sub>-N, TP and COD were measured according to “Determination of ammonia nitrogen in water quality nano reagent spectrophotometric method” (HJ 535-2009), “Determination of TP in water quality ammonium molybdate spectrophotometric method” (GB 11893-89), and “Determination of chemical oxygen demand in water quality potassium dichromate method” (HJ 827-2017), respectively. Each experiment was repeated triply and the results were averaged. The leaching efficiency and removal rate ( $\eta$ ) was calculated according to eqn (1).

$$\eta = \frac{d_0 - d_1}{d_0} \times 100\% \quad (1)$$

where  $\eta$  (%) is the leaching rate of HCl solution and HAc solution on CGCS or the removal rate of turbidity, COD, NH<sub>3</sub>-N, TP;  $d_0$  is the mass of the initial CGCS (g) or the initial concentration of turbidity (NTU), COD (mg L<sup>-1</sup>), NH<sub>3</sub>-N (mg L<sup>-1</sup>) and TP (mg L<sup>-1</sup>);  $d_1$  is the mass of CGCS after acid leaching (g) or the concentration of turbidity (NTU), COD (mg L<sup>-1</sup>), NH<sub>3</sub>-N (mg L<sup>-1</sup>) and TP (mg L<sup>-1</sup>) after treatment.



From the perspective of cost and operation efficiency, the flocculation process was carried out directly under the initial pH of riverwater, domestic sewage and aquaculture wastewater, and the dosage of PAFAC was optimized, respectively. Based on the water quality conditions, the dosage of PAFAC was set as 50, 100, 150, 200, 250, 300 mg L<sup>-1</sup> for domestic sewage and 100, 150, 200, 250, 300, 350 mg L<sup>-1</sup> for riverwater. As for aquaculture wastewater, the dosage of PAFAC was selected as 2.5, 5.0, 7.5, 10.0, 12.5 g L<sup>-1</sup>.

**2.3.2 Comparison of flocculation efficiency.** The comparison of flocculation efficiency was conducted in domestic sewage with PAFAC, flocculant A and B, in which flocculant A and B were prepared with HCl-leaching liquor and HAC-leaching liquor, respectively. The dosage of the above three flocculants was set as 250 mg L<sup>-1</sup>, and turbidity, COD, TP were introduced to evaluate the treatment efficiency. In addition, the treatment efficiency of PAFAC was further compared with those reported in the previous literature.

## 2.4 Characterization methods

XRD analysis of PAFAC was conducted on X-ray diffraction (XRD) (D8 Advance, Bruker, Germany). The parameters were set as follows: the test target was a copper target, the scanning speed was 2° min<sup>-1</sup>, and the 2θ was 5°–80°.

XRF analysis was performed on X-ray fluorescence spectrometer (Axios, Panalytical, Netherlands). The CGCS needs to be heated in a Muffle furnace (SX-G07103, Tianjin Zhonghuan Dianlu Instrument Co., Ltd, China) at 815 °C for 1.0 h to remove the carbon in it, and then its composition was determined. The flocculant can be measured directly in the instrument without high temperature calcination.

FT-IR analysis was measured on Fourier transform infrared (VERTEX70, Bruker, Germany). The sample powder was mixed with potassium bromide in a ratio of 1 : 100, and the sample was pressed into thin slices by a tablet press, which can penetrate infrared light. The thin slices were placed into the instrument for measurement. And the scanning range was 5000<sup>-1</sup>–400<sup>-1</sup>.

SEM analysis was carried out using scanning electron microscopy (SEM) (TESCAN MIRA LMS, TESCAN, Czech Republic). The sample powder was directly glued to the conductive adhesive and place on the sample table for observation. Magnification was set to 3000×, 5000× and 10 000×.

## 2.5 Mechanisms investigation

**2.5.1 Acid leaching kinetics.** In the acid leaching process, the reaction between CGCS and acid solution was mainly a solid-liquid multiphase chemical reaction between solid particles and acid solution, and the metal oxides in the solid components were gradually released by acid erosion, but insoluble minerals will eventually remain to form a loose layer. So, its kinetic behavior could be described by the unreacted shrinkage core model, which includes two cases: controlled by surface chemical reaction and controlled by loose layer diffusion. These were depicted as the following two equations (eqn (2) and (3)).<sup>21,32–35</sup>

When the acid leaching process is controlled by surface chemical reaction, the model can be expressed as:

$$1 - (1 - x)^{1/3} = K_1 t \quad (2)$$

When the acid leaching process is controlled by loose layer diffusion, the model can be expressed as:

$$1 - 3(1 - x)^{2/3} + 2(1 - x) = K_2 t \quad (3)$$

where  $x$  (%) is the leaching rate at a certain time,  $K_1$  (h<sup>-1</sup>) and  $K_2$  (h<sup>-1</sup>) are reaction rate constants and  $t$  (h) is the reaction time.

**2.5.2 Flocculation mechanisms.** Charge neutralization was investigated through zeta potential variation. The effect of variation in the dosage of flocculant on the zeta potential was investigated. 200 mL of domestic sewage was taken into a beaker, different doses (0, 50, 100, 150, 200, 250, 300 mg L<sup>-1</sup>) of flocculant were added and stirred, and the flocculation was completed and left for 15 min. Zeta potential was determined using a Zetasizer Nano ZS (Malvern Zetasizer Nano ZS, Malvern Instruments, Worcestershire, UK) at a measurement temperature of 25 °C and an equilibrium time of 30 s. The cuvette used for zeta potential measurement was a folded capillary cuvette. Each experiment was repeated three times and the results were averaged over the three experimental results.

Adsorption bridging was investigated through SEM analysis of flocculants. The flocculants were put into Scanning electron microscopy (SEM) (TESCAN MIRA LMS, TESCAN, Czech Republic) to characterize the surface structure of the flocculants, and SEM images were obtained to analyze the structure of the flocculants and the flocculation mechanism. Magnification was set to 3000×, 5000× and 10 000×.

The effect of precipitation net trapping was investigated through microscope image analysis of flocs formed by adding various dosages of PAFAC (50, 100, 150, 200, 250, 300 mg L<sup>-1</sup>) to domestic sewage (200 mL). At the end of the flocculation process, a small amount of settled floc was taken and the indicative morphology of the floc was observed by an optical microscope (B32, Chongqing OPTEC Instruments, China) with 10× magnification.

The effect of variation in the pH of domestic sewage on the flocculation efficiency was investigated, which can also show various flocculation mechanisms. The pH of domestic sewage was adjusted to 3.0, 5.0, 7.0, 9.0 and 11.0 by 1.0 mol L<sup>-1</sup> NaOH solution and 1.0 mol L<sup>-1</sup> HCl solution. Then 250 mg L<sup>-1</sup> of PAFAC was injected into 200 mL wastewater of different pH, and the removal rates of turbidity, COD, and TP were calculated after the completion of flocculation to explain the effect of pH of wastewater on flocculation.

## 3. Results and discussion

### 3.1 Acid leaching process investigations

As shown in Fig. 2A, when the concentration of HCl solution was increased from 1.0 mol L<sup>-1</sup> to 3.0 mol L<sup>-1</sup>, the leaching efficiency was promoted from 26.74% to 85.76%. As the concentration of acid was increased, the concentration of H<sup>+</sup>





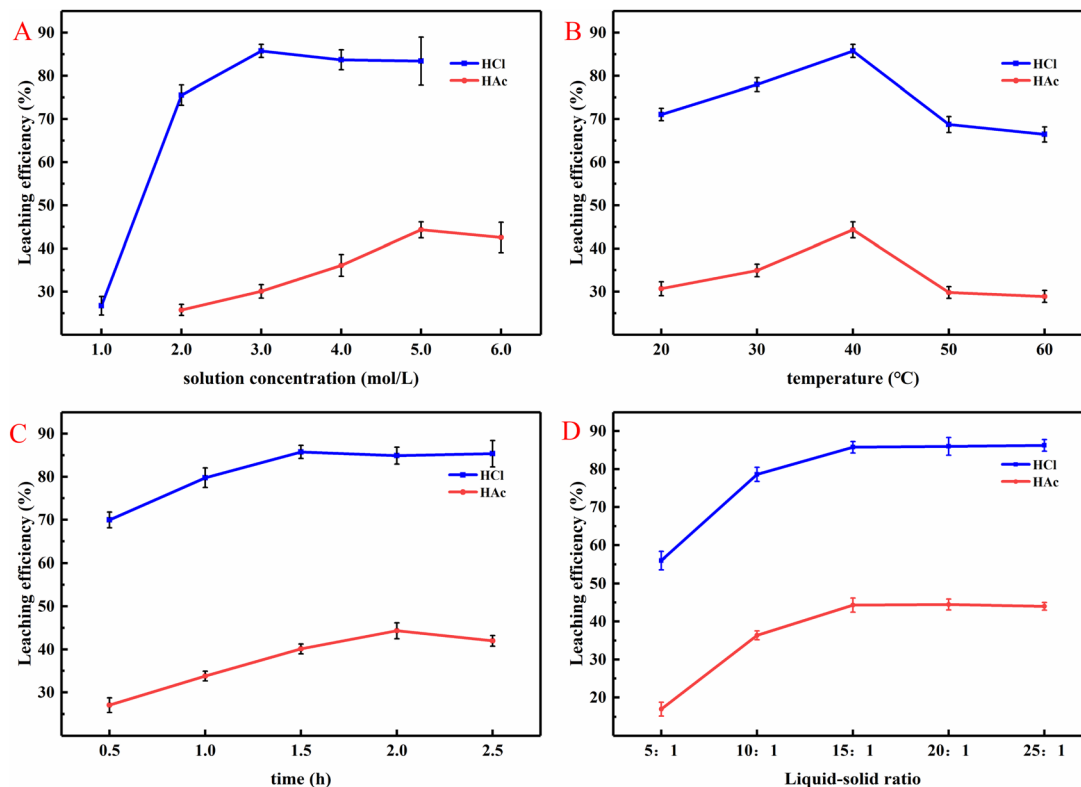


Fig. 2 Effect of various acid leaching conditions on acid leaching efficiency. (A) Acid concentration, (B) temperature, (C) time, (D) liquid–solid ratio.

was continuously increased, which promoted the full reaction with the CGCS, and led to the increase of leaching efficiency. The leaching efficiency remained essentially unchanged after the concentration increased to  $4.0 \text{ mol L}^{-1}$  and  $5.0 \text{ mol L}^{-1}$ , suggesting that a sufficient concentration of  $\text{H}^+$  was provided at a concentration of  $3.0 \text{ mol L}^{-1}$  in the HCl solution. The leaching efficiency increased from 25.77% to 44.32% when the concentration of HAc solution was increased from  $2.0 \text{ mol L}^{-1}$  to  $5.0 \text{ mol L}^{-1}$  and the elevated concentration of  $\text{H}^+$  enhanced the efficiency of metal elements leaching. The leaching efficiency was almost unchanged when the concentration was increased to  $6.0 \text{ mol L}^{-1}$ , indicating that sufficient  $\text{H}^+$  had been provided at the HAc solution concentration of  $5.0 \text{ mol L}^{-1}$ . Therefore, for acid leaching of CGCS, the concentration of HCl solution was selected as  $3.0 \text{ mol L}^{-1}$  and the concentration of HAc solution was selected as  $5.0 \text{ mol L}^{-1}$ .

As shown in Fig. 2B, in the range of  $20\text{--}40^\circ\text{C}$ , the acid leaching efficiency of HCl and HAc solution increased from 71.07% to 85.76% and 30.70% to 44.32%, respectively, the results indicated that the increasing temperature could improve the efficiency of leaching metal elements from CGCS.<sup>36</sup> However, when the temperature was raised to  $50^\circ\text{C}$ , the acid leaching efficiency of HCl and HAc solution was reduced to 68.73% and 29.83%, and at the temperature of  $60^\circ\text{C}$ , the leaching efficiency of HCl and HAc solution was similar to that at  $50^\circ\text{C}$  and also had a weak trend of decline. It was attributed that the final acid leaching liquor would produce colloidal

substances, and wrapped in the surface of the CGCS at higher acid leaching temperature, resulting in the difficulty of the solid–liquid separation. On the other hand, the high temperature would make the acid leaching liquor speed up the auto-polymerization reaction, inhibiting the leaching of metal oxides inside CGCS.<sup>37</sup> Therefore, considering the leaching efficiency and economic benefits, the optimal acid leaching temperature of both HCl and HAc was selected as  $40^\circ\text{C}$ .

In Fig. 2C, it was found that the acid leaching efficiency of HCl solution increased from 75.28% to 85.76% in the range of 0.5 h to 1.5 h, while the leaching efficiency was almost unchanged when the time was prolonged from 2.0 h to 2.5 h. The acid leaching efficiency increased from 27.04% to 44.32% when HAc acid leaching time was in the range from 0.5 h to 2.0 h. When the time was increased to 2.5 h, the leaching efficiency was almost unchanged. The results showed that the acid leaching reaction had almost reached equilibrium in 1.5 h of HCl-leaching process and 2.0 h of HAc-leaching process, the acid leaching reaction had almost reached equilibrium. With the prolongation of the reaction time, the acid leaching solution would take auto-polymerization,<sup>37</sup> leading to the colloidal substances attached to the remaining CGCS, and increasing the difficulty of solid–liquid separation. Therefore, the optimal acid leaching time of HCl and HAc was 1.5 h and 2.0 h, respectively.

In Fig. 2D, when the liquid–solid ratio increased from 5 : 1 to 15 : 1, the leaching efficiencies of HCl and HAc increased from 55.96% to 85.76% and 16.96% to 44.32%, respectively, and then



stabilized after increasing the ratio again. It could be found that when the liquid–solid ratio reached 15 : 1, the upper limit of acid leaching efficiency of metal elements had basically been reached, and the  $H^+$  in the acid had already been fully utilized.<sup>36</sup> So, the optimal liquid–solid ratios for acid leaching of both HCl and HAc were chosen as 15 : 1.

### 3.2 Preparation of PAFAC

**3.2.1 Effect of acid leaching liquor volume ratio of HCl to HAc.** As shown in Fig. 3A, it was found that the minimum turbidity occurred at the dosage of PAFAC of 20 mg L<sup>-1</sup>. The results indicated that excessive flocculant might wrap the same charge colloidal particles and repel each other, resulting in a destabilized state.<sup>38</sup>

Fig. 3B exhibited the removal efficiency of turbidity of kaolin wastewater by PAFAC with different volume ratios at a flocculant dosage of 20 mg L<sup>-1</sup>. When the volume ratio increased from 5 : 1 to 3 : 2, the residual turbidity was reduced from 53.64 NTU to 28.66 NTU, and the removal efficiency was increased from 93.90% to 97.01%. As the HAc-leaching liquor continued to increase, the volume ratio decreased from 3 : 2 to 2 : 3. The residual turbidity increased to 151.91 NTU and the removal efficiency decreased to 84.15%. The optimal volume ratio of 3 : 2 was chosen for the preparation of PAFAC.

**3.2.2 Effect of polymerization pH.** Fig. 4A exhibited the effect of polymerization pH on the turbidity removal of kaolin wastewater. When the pH was 2.0, the residual turbidity was 89.28 NTU and the removal rate was 90.68%, when the pH was

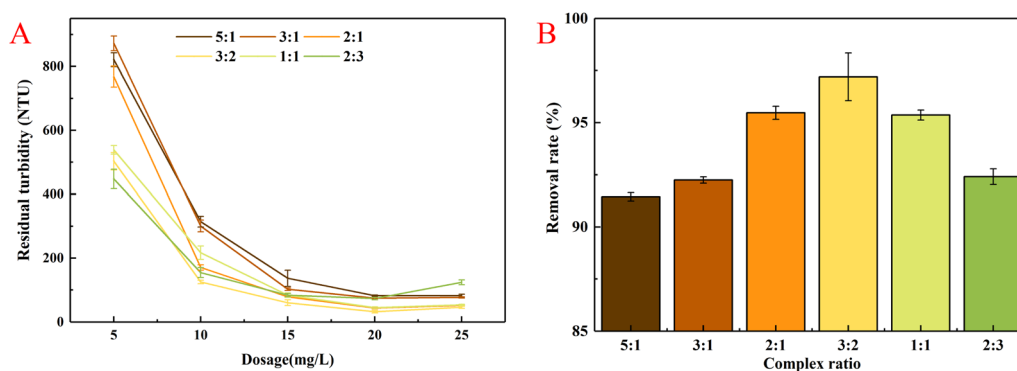


Fig. 3 Effect of volume ratio: (A) residual turbidity, (B) removal rate.

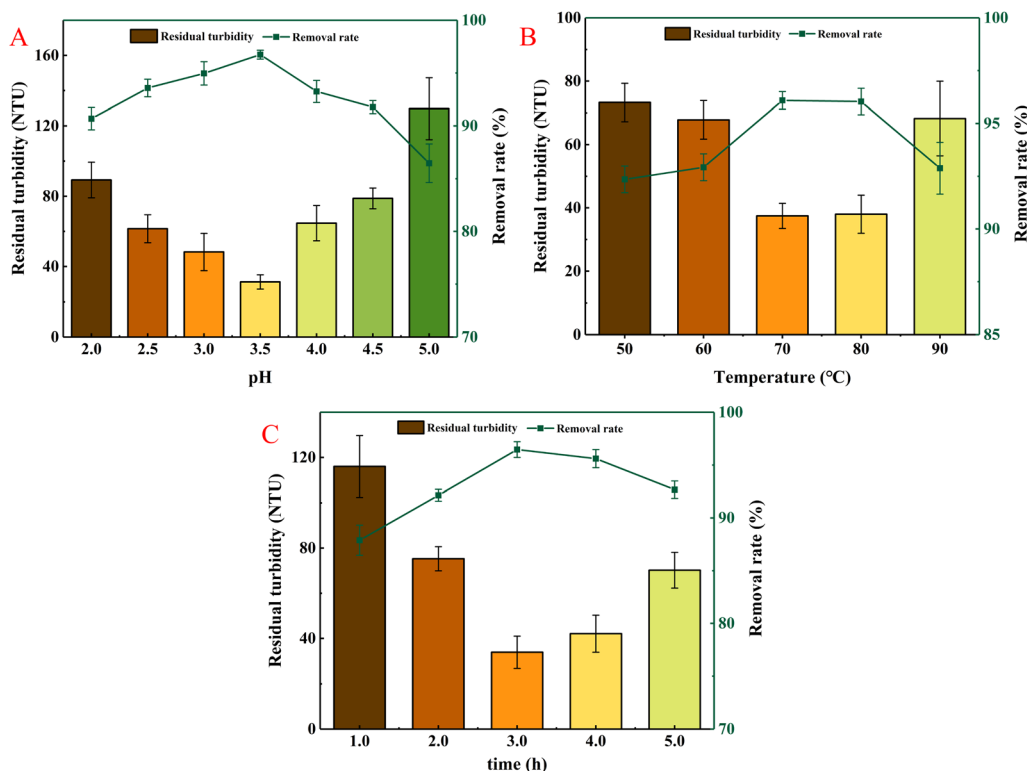


Fig. 4 Effect of factors on removal efficiency. (A) Polymerization pH, (B) reaction temperature, (C) reaction time.



increased to 3.5, the residual turbidity was reduced to 31.22 NTU and the removal rate was increased to 96.74%, but as the pH was increased to 5.0, the residual turbidity was rapidly increased to 129.75 NTU and the removal rate was rapidly reduced to 86.46%. This was mainly because, with the increase of pH, the  $\text{OH}^-$  in the system increased, promoting Fe and Al to polymerize into multinucleated hydroxyl complexes and modifying the flocculation efficiency.<sup>39</sup> However, with the increasing pH, the increasing  $\text{OH}^-$  might lead to the precipitation of Fe and Al, reducing the stability of the flocculant.<sup>40</sup> Therefore, the optimal pH was selected as 3.5.

**3.2.3 Effect of reaction temperature.** As shown in Fig. 4B, it could be seen that when the temperature was below 70 °C, the removal ability of turbidity of kaolin wastewater increased with the increase of temperature, and at 70 °C, the residual turbidity was reduced to 33.78 NTU, and the removal rate was increased to 96.48%. The results showed that lower temperature was not conducive to hydrolysis polymerization, and the reaction time may be longer. Therefore, the reaction was not fully balanced at lower reaction temperature, and the flocculation ability of the obtained PAFAC was weakened.<sup>41</sup> When the temperature was increased to 80 °C, the removal ability of PAFAC on the turbidity of kaolin wastewater was almost unchanged, which indicated that the equilibrium of the hydrolysis polymerization reaction had been reached at the reaction temperature of 70 °C. When the reaction temperature was higher than 80 °C, the performance of the synthetic flocculant decreased due to the hydrolysis and precipitation of  $\text{Fe}^{3+}$  and  $\text{Al}^{3+}$  in the solution.<sup>42</sup>

**3.2.4 Effect of reaction time.** As shown in Fig. 4C, the removal ability of PAFAC on the turbidity of kaolin wastewater increased rapidly when the reaction time increased. The results indicated that the reaction rate was faster in the pre-reaction stage. At the reaction time of 3.0 h, the residual turbidity decreased to 33.92 NTU and the removal rate increased to 96.46%. The reaction time extended from 3.0 h to 5.0 h, and the removal ability of PAFAC on the turbidity of kaolin wastewater decreased slowly, which demonstrated that the hydroxyl group would continue to react with  $\text{Fe}^{3+}$  and  $\text{Al}^{3+}$  and form the precipitation, reducing the flocculation efficiency.<sup>21</sup>

### 3.3 Characterization of PAFAC

Tables 2 and 3 are the component analysis results of CGCS and PAFAC by XRF, respectively. As depicted in Table 2, it could be seen that CGCS was mainly composed of  $\text{SiO}_2$ ,  $\text{Fe}_2\text{O}_3$ ,  $\text{Al}_2\text{O}_3$ , and CaO. The results revealed that CGCS had the effective ingredients for flocculant preparation.

Table 3 showed that PAFAC was a polyionic composite flocculant including Fe, Al, and Ca. The existence of Na came from NaOH that was utilized to adjust pH during the preparation process and formed NaCl crystal with  $\text{Cl}^-$  of HCl, which is also presented in the XRD patterns of Fig. 5A. According to Tables 2 and 3, the metal elements in the CGCS had been leached out by HCl solution and HAc solution effectively.

In Fig. 5A, only the diffraction peak of NaCl was observed when the volume ratio was in the range from 5 : 1 to 3 : 2. The results revealed that PAFAC might be a kind of amorphous polymer. With the further increase of the HAc-leaching liquor, namely the volume ratio reached 1 : 1 and 2 : 3, it was found that some stray peaks appeared in the range of 10°–30°, which indicated that the addition of too much HAc leaching liquor would lead to the precipitation of some crystalline salts and thus reduce the flocculation efficiency. The result was in good agreement with the results described in Fig. 3.

FT-IR spectra of PAFAC with different volume ratios were demonstrated in Fig. 5B. The bands at 3400  $\text{cm}^{-1}$  and 1628  $\text{cm}^{-1}$  could attributed to the  $\text{OH}^-$  vibration of Al-OH, Fe-OH and H-OH.<sup>43</sup> The peaks intensity reached the maximum at the volume ratio of 3 : 2. The results suggested that the amount of ligand water of Al-Fe hydroxylated copolymers in PAFAC reached the maximum, the strongest bonding interactions with the central ions after transformation into structured water, which was one of the reasons why PAFAC achieved the best flocculation efficiency at a ratio of 3 : 2.<sup>44</sup> A weaker characteristic peak at 920–1068  $\text{cm}^{-1}$  might be assigned to the stretching vibration of Fe-O-Fe and Al-O-Al bonds.<sup>45</sup> The bands of 478  $\text{cm}^{-1}$ –515  $\text{cm}^{-1}$  could be the bending vibrations of Fe-O and Al-O.<sup>46</sup> The appearance of the characteristic peak at 1473  $\text{cm}^{-1}$  could be due to the asymmetric scaling of the carboxylate group ( $-\text{COO}^-$ ). The intensity of this peak increased significantly with the increase of HAC-

Table 2 Component analysis of CGCS by XRF

Samples	Component analysis										
	$\text{SiO}_2$	$\text{Fe}_2\text{O}_3$	$\text{Al}_2\text{O}_3$	CaO	$\text{Na}_2\text{O}$	$\text{SO}_3$	$\text{TiO}_2$	$\text{K}_2\text{O}$	MgO	BaO	Others
Content (%)	42.95	15.26	16.47	17.26	2.52	1.65	1.11	0.97	0.58	0.26	0.97

Table 3 Component analysis of PAFAC by XRF

Samples	Component analysis									
	Fe	Al	Ca	Si	K	Mg	Ti	Na	Cl	Others
Content (%)	13.95	7.58	11.79	5.89	1.21	0.74	0.39	14.24	42.08	2.13

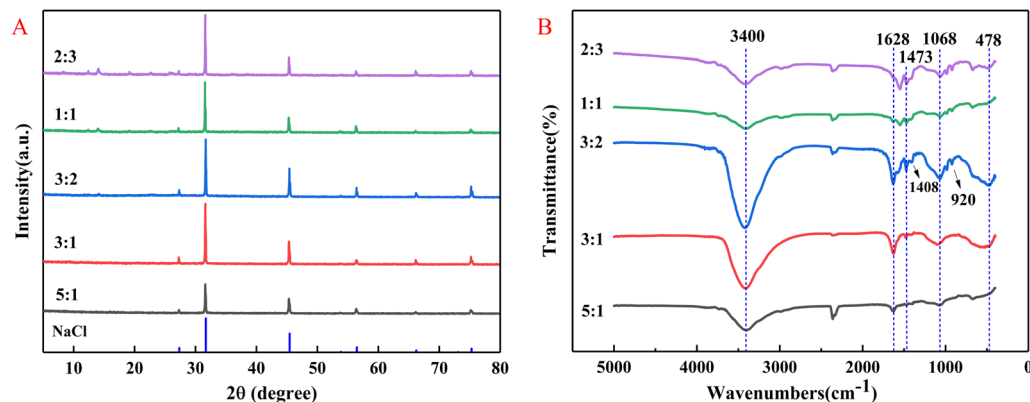


Fig. 5 Characterization of PAFAC. (A) XRD, (B) FTIR.

leaching liquor compared to that occurred at the volume ratios of 5:1 and 3:1, proving that it was associated with  $\text{COO}^-$ . The characteristic peak appeared at  $1408\text{ cm}^{-1}$  when the ratio was 3:2–2:3, which was attributed to the coordination interactions between the metal ions and  $\text{COO}^-$  groups in PAFAC.<sup>47</sup> Overall, the intensity of the characteristic peaks of PAFAC was significantly stronger at the volume ratio of 3:2 than those of the other ratios, which indicated that a suitable complex ratio could increase the degree of polymerization of PAFAC.<sup>30</sup>

### 3.4 Performance of PAFAC on real wastewater treatment

#### 3.4.1 Dosage effect of PAFAC on flocculation efficiency. In

Fig. 6A, it could be seen that the highest treatment efficiency of turbidity, COD and TP occurred at the dosage of  $250\text{ mg L}^{-1}$ , which resulted in 89.62% removal of turbidity, 58.95% of COD, and 76.76% of TP. However, it could be seen that the removal of  $\text{NH}_3\text{-N}$  was less than 10% at any dosage. These results might be attributed that most of the ammonium salts in domestic sewage were in water-soluble form, and flocculants mainly played

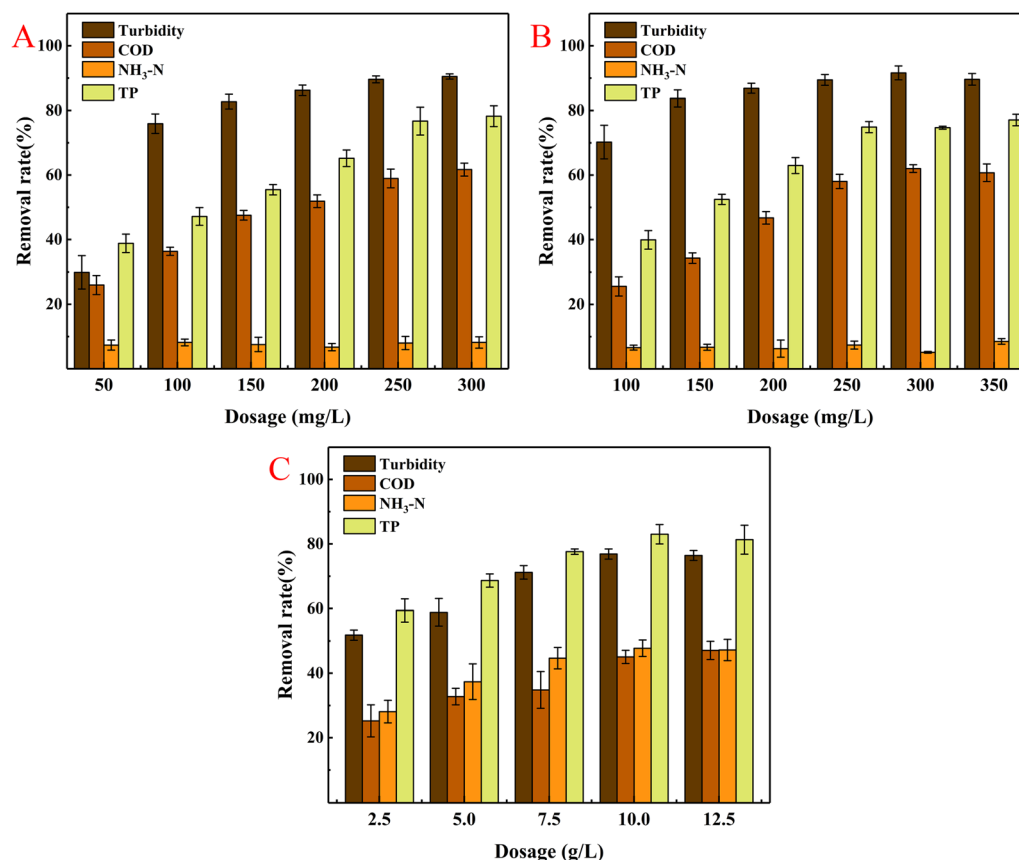


Fig. 6 Effectiveness in treating pollutants in various water bodies. (A) Domestic sewage, (B) river water, (C) aquaculture wastewater.





a great role in the removal of suspended and colloidal particles, so the removal of  $\text{NH}_3\text{-N}$  from domestic sewage by PAFAC was extremely low. Whereas PAFAC showed great treatment efficiency for removing turbidity, COD and TP in domestic sewage.

As shown in Fig. 6B, the optimal treatment efficiency occurred at a  $300 \text{ mg L}^{-1}$  dosage. However, the improvement of the removal efficiency was not significant compared with that at  $250 \text{ mg L}^{-1}$ . Considering the cost-effectiveness, the optimal dosage of PAFAC was selected as  $250 \text{ mg L}^{-1}$ .

As shown in Fig. 6C, the removal rate of pollutants basically reached the maximum at the dosage of  $10 \text{ g L}^{-1}$ , the removal of turbidity was of 76.89%, COD of 45.09%,  $\text{NH}_3\text{-N}$  of 47.76% and TP of 83.02%. The results indicated that the removal capacity of  $\text{NH}_3\text{-N}$  by PAFAC was improved, which could be attributed that the physicochemical properties of aquaculture wastewater were different from those of domestic sewage and riverwater, and some of the  $\text{NH}_3\text{-N}$  presented in aquaculture wastewater might be the form of particles or colloids, so PAFAC was much more effective in treating  $\text{NH}_3\text{-N}$  in aquaculture wastewater than that of domestic sewage and riverwater.

**3.4.2 Comparison of the flocculation efficiency.** Fig. 7 showed the flocculation efficiency of PAFAC, flocculant A

(prepared from the HCl-leaching liquor) and flocculant B (prepared from HAc-leaching liquor) on domestic sewage. It was found that PAFAC had a better removal effect than those of flocculant A and flocculant B, and the removal efficiency of turbidity, COD and TP, which was up to 91.42%, 59.94% and 78.77%, respectively. The results further revealed that the two-step acid leaching process was more effective than the one-step acid leaching process. It was found that the introduction of  $\text{CH}_3\text{COO}^-$  played a significant role in promoting molecular weight, improving the flocculation efficiency.<sup>48</sup>

Furthermore, the treatment efficiency of turbidity of PAFAC was compared with other flocculants reported in the previous research.<sup>21,49–55</sup> As shown in Table 4, it could be found that PAFAC was feasible for the synthesis of flocculant, which showed good performance for the removal of turbidity.

## 4. Investigations on mechanisms

### 4.1 Acid leaching kinetics

The results of acid leaching kinetics were investigated in Fig. 8 and Table 5. From Fig. 8A and B, it could be seen that “ $1 - (1 - x)^{1/3}$ ” and “ $1 - 3(1 - x)^{2/3} + 2(1 - x)$ ” had a good linear relationship with “ $t$ ” in the acid leaching process of HCl and HAc in the range of 0.5 h–2.5 h. The fitted  $R^2$  of the two kinetic equations corresponding to HCl-acid leaching were 0.83 and 0.85, and the fitted  $R^2$  of the two kinetic equations corresponding to HAc-acid leaching were 0.90 and 0.93, respectively. However, since the leaching rate was maximized at 1.5 h for HCl-acid leaching and at 2.0 h for HAc-acid leaching, the  $\text{H}^+$  in the acid was fully utilized, and the reaction was complete. The following reasons could explain the above phenomenon: with the extension of the reaction time, the acid leaching liquor had a tendency to polymerize, and the colloidal substance produced by polymerization adhered to the surface of CGCS, affecting the diffusion of the acid and its contact with CGCS, and the acid soak activity was not effectively carried out in the subsequent time range.<sup>21</sup> To further reveal the acid leaching kinetics, the model of “ $1 - (1 - x)^{1/3}$ ” and “ $1 - 3(1 - x)^{2/3} + 2(1 - x)$ ” versus “ $t$ ” during HCl-acid leaching in the range of 0.1 h to 1.5 h, and “ $1 - (1 - x)^{1/3}$ ” and “ $1 - 3(1 - x)^{2/3} + 2(1 - x)$ ” versus “ $t$ ” during HAc-acid leaching in the range of 0.25 h to 2.0 h were investigated, respectively (Fig. 8C and D). It could be seen that both “1

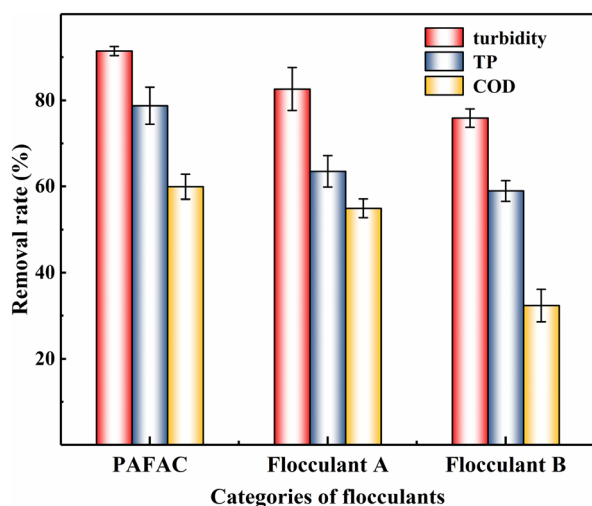


Fig. 7 Comparison of the treatment efficiency.

Table 4 Comparison of the treatment efficiency

Types of flocculants	$C_0$ (NTU)	$C_1$ (NTU)	Dosage ( $\text{mg L}^{-1}$ )	Removal rate (%)
PSBFZ- $\text{Fe}_3\text{O}_4$ (ref. 49)	20–25	0.8–1.0	300	96.00
Coagulant-3.0 (ref. 21)	2104	42.08	100	98.00
Al- $\text{P}^{50}$	707	8.48	14	98.80
YCW-PAC <sup>51</sup>	100	2.0	300	98.00
CMCNa <sup>52</sup>	33	2.31	100	93.00
XCTS <sup>53</sup>	200	28.20	90	85.90
XG- $\text{Fe}(\text{III})$ <sup>54</sup>	3247	31.5	20	99.03
PSTF <sup>55</sup>	700	33.60	45	98.20
PAFAC	958.40	28.66	20	97.01



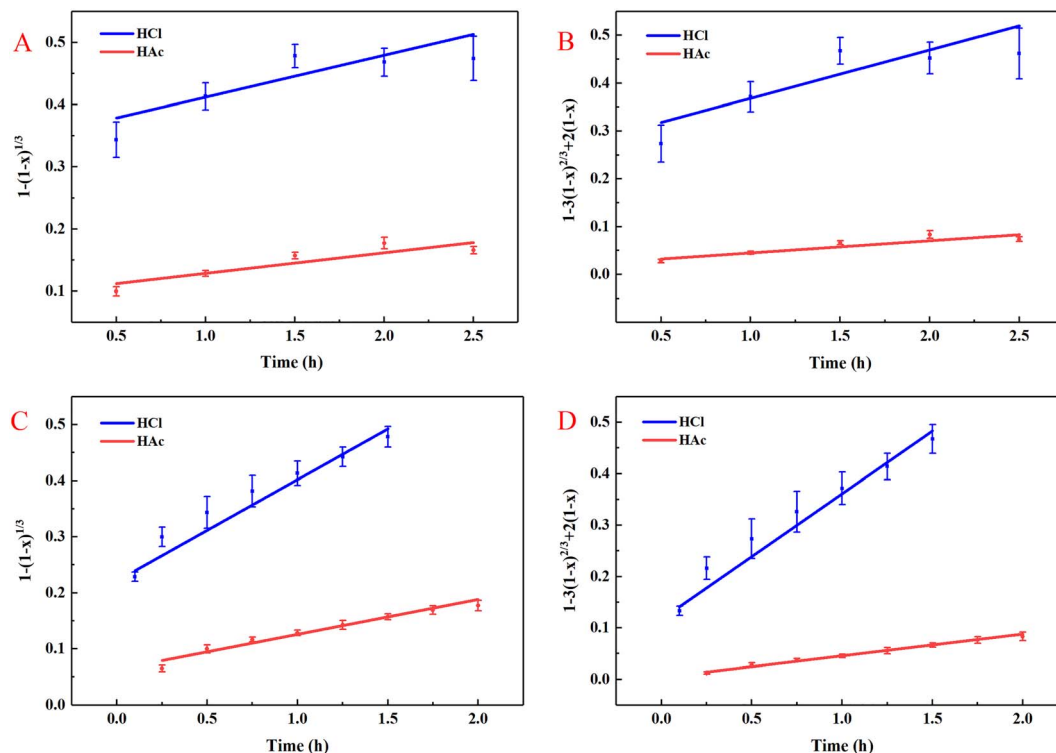


Fig. 8 Acid leaching kinetics. (A and C) Linear relationship between " $1 - (1 - x)^{1/3}$ " and " $t$ ", (B and D) linear relationship between " $1 - 3(1 - x)^{2/3} + 2(1 - x)$ " and " $t$ ".

Table 5 Rate constants of kinetics models and correlation coefficients in the acid leaching process

Types of acids	Kinetics model and the relative parameters			
	Surface chemical reaction		Diffusion through the product layer	
	$1 - (1 - x)^{1/3}$		$1 - 3(1 - x)^{2/3} + 2(1 - x)$	
	$K_1$	$R^2$	$K_2$	$R^2$
A: HCl	$6.725 \times 10^{-2}$	0.83388	$10.096 \times 10^{-2}$	0.84845
B: HAc	$3.306 \times 10^{-2}$	0.90246	$2.544 \times 10^{-2}$	0.9326
C: HCl	$18.058 \times 10^{-2}$	0.98402	$24.423 \times 10^{-2}$	0.98897
D: HAc	$6.231 \times 10^{-2}$	0.9764	$4.211 \times 10^{-2}$	0.99453

$1 - (1 - x)^{1/3}$  and " $1 - 3(1 - x)^{2/3} + 2(1 - x)$ " had a highly linear relationship with " $t$ ", and the  $R^2$  of both models for the HCl-acid leaching were more than 0.98, and which of HAc-acid leaching also reached 0.97 and 0.99, respectively. The results showed that the unreacted shrinkage core model was in good agreement with the acid leaching process, and the acid leaching process involved both surface chemical reaction and loose layer diffusion.<sup>32</sup>

To further investigate the acid leaching mechanism, the SEM images of the original CGCS and its residues after HCl and HAc acid leaching were demonstrated in Fig. 9. It was found that the surface of the original CGCS was covered with  $\text{SiO}_2$  microspheres and various metal oxides but few pores

(Fig. 9A and D). With the time going on, it could be seen that the surface of the CGCS gradually became rough due to the opened pores (Fig. 9B and E). Then the acid started to diffuse into the interior of the pores, react with the metal oxides of looser layer, leaving the smoother inner surface and larger pore size (Fig. 9C and F), which played a significant role in enhancing the acid leaching efficiency. The results were in good agreement with surface chemical reaction and loose layer diffusion, greatly supporting the mechanisms of acid leaching.

## 4.2 Flocculation mechanism of PAFAC

The flocculation mechanism of PAFAC includes electric neutralization, adsorption bridging and precipitation net trapping. Fig. 14 is a schematic diagram of the overall flocculation mechanism of PAFAC.

**4.2.1 Charge neutralization.** Fig. 10 showed the effect of PAFAC dosage on the zeta potential of domestic sewage after flocculation. It could be attributed that zeta potential gradually decreased with the increase of the dosage, which indicated that charge neutralization played a role in the flocculation process of PAFAC. It could be deduced that PAFAC might hydrolyze and bring positive ions with the increase in the amount of dosage and produce electrostatic attraction with the negative charge on the surface of the colloidal particles, making the colloidal surface potential decrease, and colloidal particles in the electrostatic attraction of the cohesion in the continuous destabilization of sinking.<sup>50,56</sup> However, at the



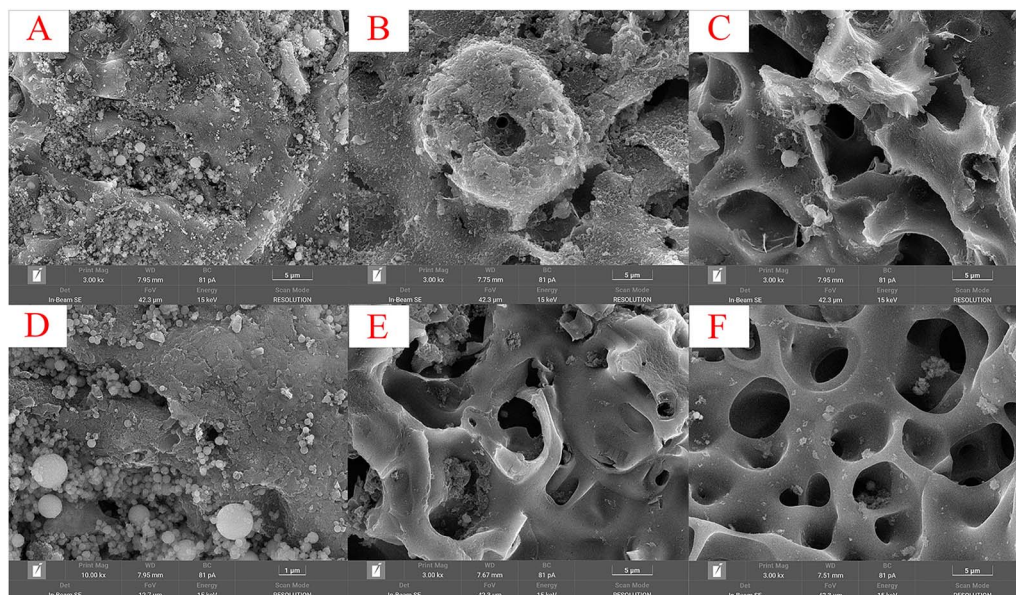


Fig. 9 SEM of the original CGCS and CGCS in the process of acid leaching. (A and D) Original CGCS with magnification of 3000 $\times$  and 10 000 $\times$ ; (B and C) HCl-acid leaching for 0.5 h and 1.5 h with magnification of 3000 $\times$ ; (E and F) HAC-acid leaching for 1.0 h and 2.0 h with magnification of 3000 $\times$ .

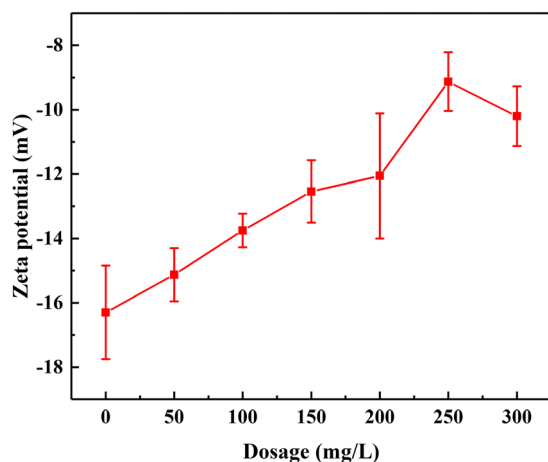


Fig. 10 PAFAC dosage effect on zeta potential of domestic sewage.

dosage of 250 mg L<sup>-1</sup>, the zeta potential had not yet reached the zero point. Then continued to increase the dosage to 300 mg L<sup>-1</sup>, the zeta potential began to increase and the flocculation efficiency of turbidity, COD and TP of domestic sewage was basically unchanged and only a weak trend to increase, all of which indicated that other flocculation mechanisms might also play an important role in the flocculation process.<sup>56,57</sup>

**4.2.2 Adsorption bridging.** From Fig. 11A, it could be seen that flocculant A had abundant pores with a large specific surface area, which was conducive to the adsorption bridging effect of the flocculant on the colloid and suspended matter.<sup>58</sup> However, its looser structure had some limitations on the flocculation efficiency. As shown in Fig. 11B, it was found that flocculant B had the morphology of bars and

branch chains, and the structure could enhance the ability of adsorption and net trapping, which was conducive to the sedimentation of flocs. Moreover, Fig. 11C and D further revealed that PAFAC had a tight and complex gel network structure, which possessed the pore structure of flocculant A of tiny pores and the branch structure of flocculant B of interlaced branch chains, forming a compact and complex gel network structure of PAFAC and contributing to the direct bridging of colloidal particles and flocs.<sup>59</sup> Fig. 11E and F was the EDS elemental mapping diagram of PAFAC. It can be seen that elements such as Fe and Al are well distributed on the surface of PAFAC, which is conducive to the full combination of metal elements such as Fe and Al with pollutants after hydrolysis, so as to effectively remove pollutants. In addition, the surface of PAFAC also had more folds, which resulting in a coarser surface and larger specific surface area than the other two flocculants, improving the flocculation performance.<sup>60</sup>

**4.2.3 Precipitation net trapping.** As could be seen from Fig. 12, with the increase of the dosage, the architecture of the floc gradually changed from a loose structure to a compact and dense one. It was because the polymer extended the branch chains by adsorption bridging, and then extended the branch chains around other unabsorbed particles by the long chain net and sank together, and finally linked the particles together to form aggregates.<sup>61</sup> Therefore, with the less flocculant, the adsorption bridging and precipitation net trapping would not work, and the aggregates would be loose. When the dosage increased to 300 mg L<sup>-1</sup>, there was a tendency for the floc to change from a compact structure to a loose structure, which indicated that the excessive dosage would result in an excess of unneutralized sites and cause the floc surface to become



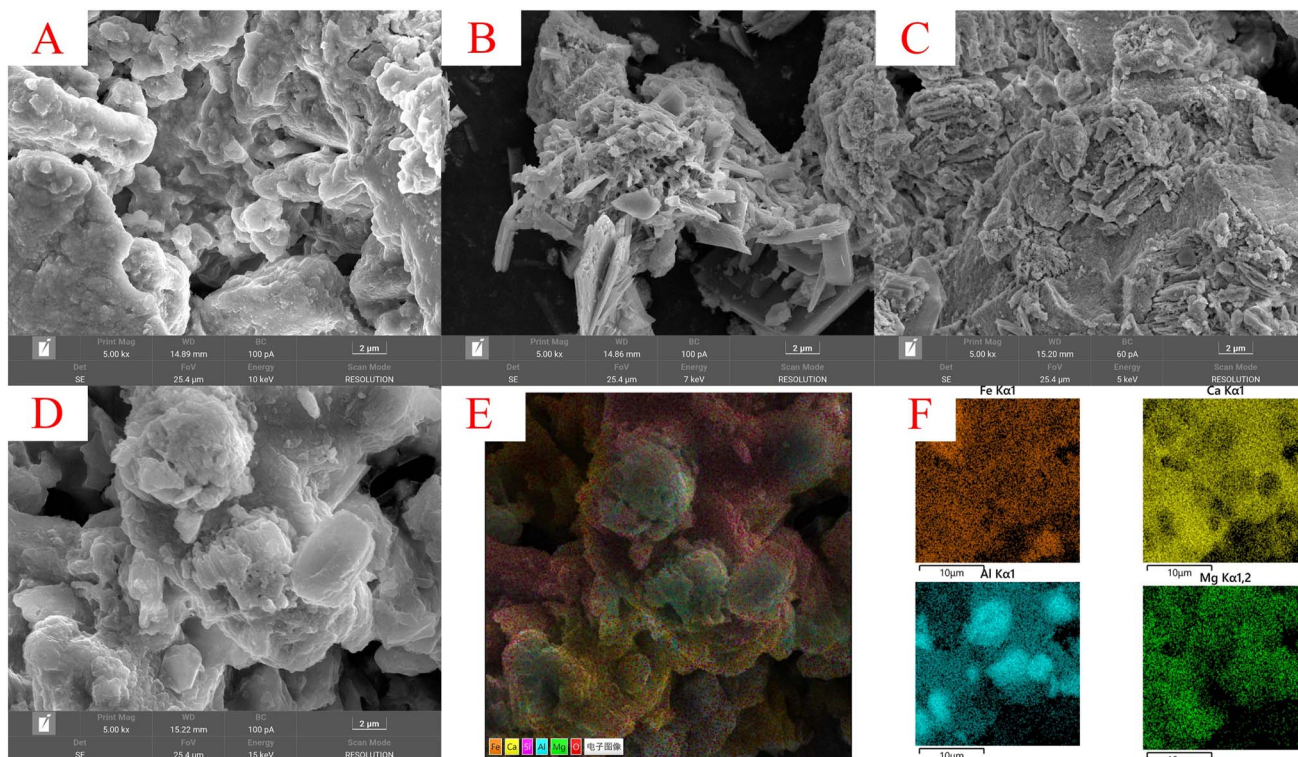


Fig. 11 SEM image of (A) flocculant A with magnification of 5000 $\times$ ; (B) flocculant B with magnification of 5000 $\times$ ; (C and D) PAFAC with magnification of 5000 $\times$ ; (E and F) EDS elemental mapping of PAFAC.

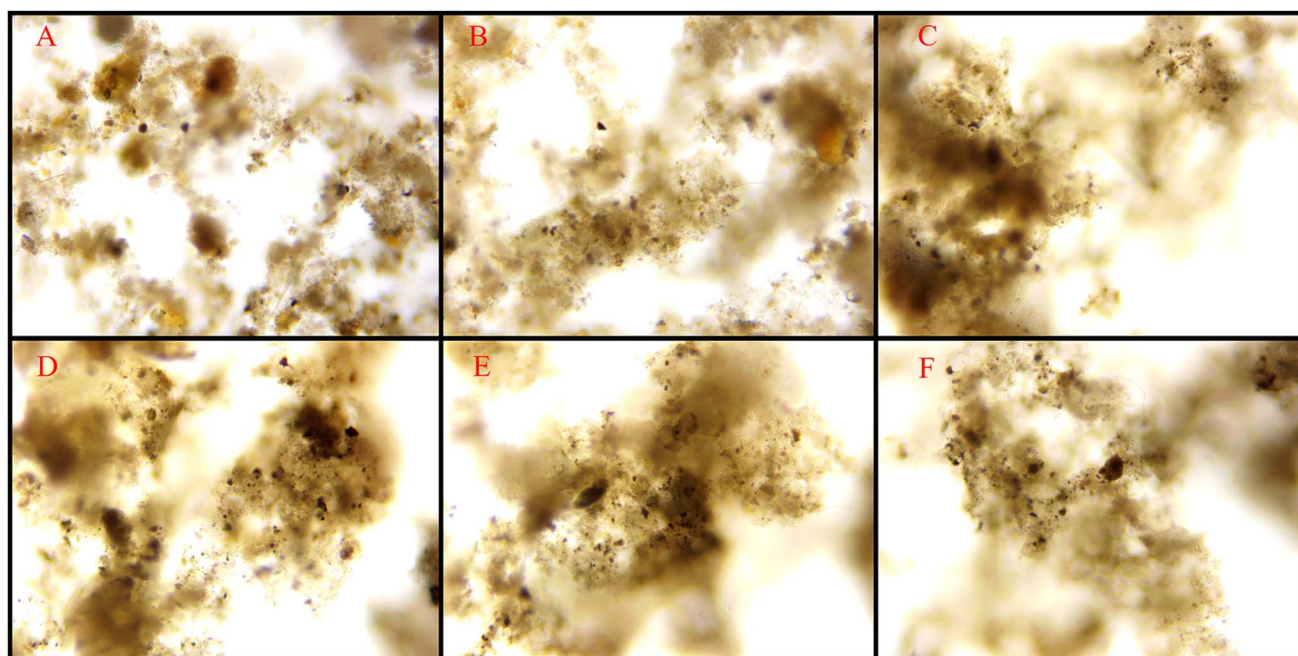


Fig. 12 Optical microscope images of flocs. (A), (B), (C), (D), (E) and (F) are the images at dosages of 50, 100, 150, 200, 250 and 300 mg L<sup>-1</sup>, respectively.

negatively charged again and produce a repulsive force, thus weaken the effect of charge neutralization.<sup>62</sup> However, according to the experiment, the flocculation effect was not

weakened when the dosage was 300 mg L<sup>-1</sup>, which indicated that both adsorption bridging and precipitation net trapping played an important role in the flocculation process of



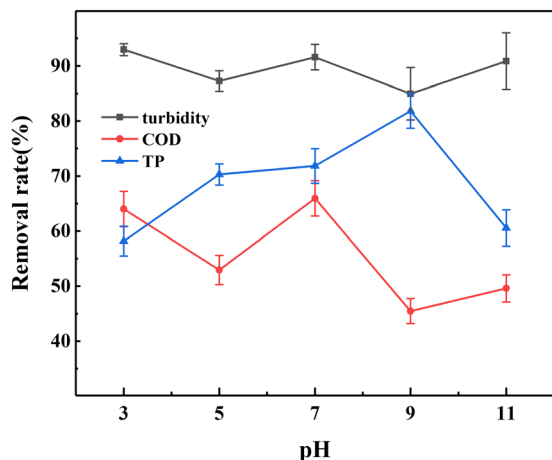


Fig. 13 Effect of wastewater pH on flocculation efficiency.

PAFAC.<sup>63</sup> The flocs after flocculation showed a floc cross-linking structure, which further also indicated that the presence of adsorption bridging and precipitation net trapping causes the particles to interact with each other and eventually agglomerate and sink.<sup>50</sup>

In addition, the effect of pH was investigated to further reveal the treatment efficiency of turbidity, COD and TP. As shown in Fig. 13, the good removal effect at pH 3.0 was attributed that metal ions ( $\text{Al}^{3+}$ ,  $\text{Fe}^{3+}$ ,  $\text{Ca}^{2+}$ , etc.) of PAFAC were hydrolyzed into mononuclear and polynuclear hydroxyl complex ions under the strong acid environment, which adsorbed suspended colloidal particles in the system and rapidly aggregate to form large and dense flocs.<sup>21,64</sup> At pH 7.0, the flocculation performance was mainly based on

adsorption bridging, supplemented by charge neutralization, and in this way, the flocculant also possessed good removal performance.<sup>65</sup> However, at pH 5.0, charge neutralization was not as strong as strong acid conditions, and adsorption bridging was not as strong as neutral conditions, resulting a weaker flocculation performance.<sup>66</sup> When the pH was increased to 9.0, the removal efficiency of the flocculant on turbidity and COD decreased sharply to 84.95% and 45.47%. This was because the rate and degree of hydrolysis of  $\text{Fe}^{3+}$  and  $\text{Al}^{3+}$  was intensified in an alkaline environment, which tended to form  $\text{Fe}(\text{OH})_3$  and  $\text{Al}(\text{OH})_3$  precipitates, thus weakening the performance of PAFAC and led to a significant decrease in flocculation effect.<sup>67</sup> When the pH was increased to 11.0,  $\text{OH}^-$  increased, and some pollutants in domestic sewage would react with  $\text{OH}^-$  to form precipitation, which made it easier for the pollutants to settle through precipitation net trapping with PAFAC. However, at pH 11.0, the removal rate of COD did not increase as significantly as that of turbidity due to the hydrolysis of  $\text{Fe}^{3+}$  and  $\text{Al}^{3+}$  further aggravated in the strong alkali environment, which weakened the flocculant performance and decreased the efficiency of COD removal.

It was found that the removal efficiency of TP improved with the increase of pH, which reached its maximum of 81.84% at pH 9.0. The results indicated that  $\text{PO}_4^{3-}$  in solution would exchange ligands with the  $-\text{OH}/-\text{OH}_2$  groups of Al and Fe to form  $\text{AlPO}_4$  and  $\text{FePO}_4$  precipitates or similar Al-P and Fe-P compounds in neutral and partially neutral environments, which is conducive to the removal of  $\text{PO}_4^{3-}$ .<sup>68</sup> The removal efficiency of TP was weak at pH 3.0 and 11.0 because the phosphate might dissolve under strongly acidic or alkaline environments.<sup>69</sup>

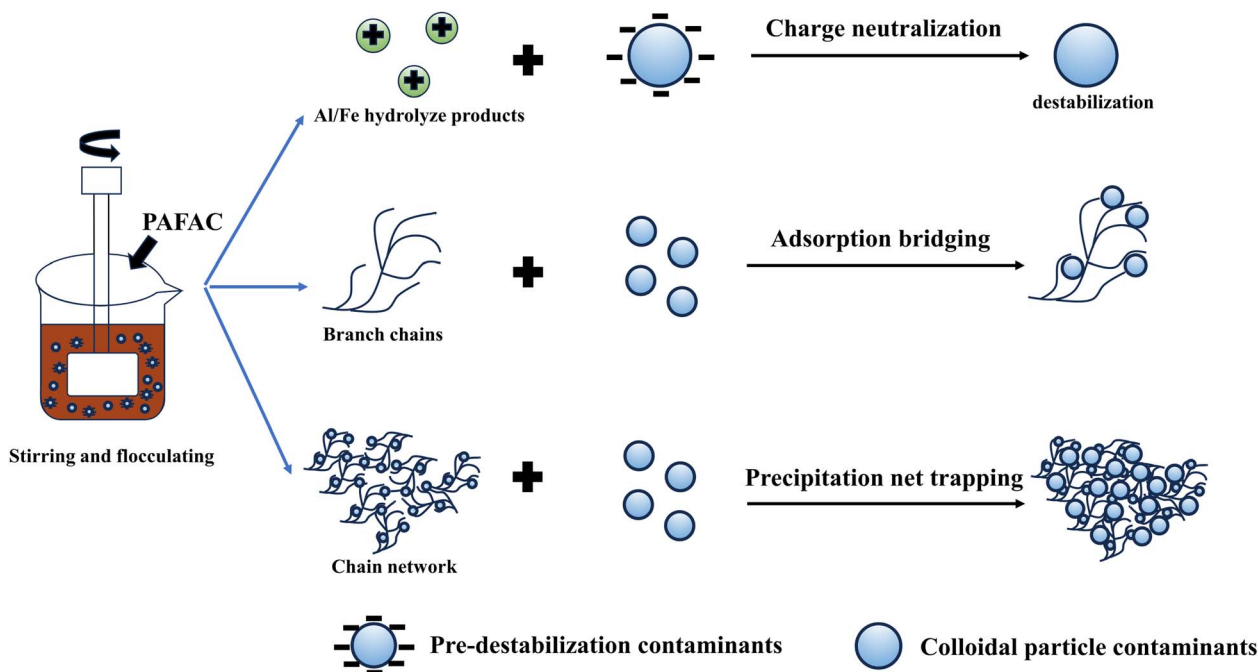


Fig. 14 The schematic diagram of flocculation mechanism of PAFAC.



## 5 Conclusion

In the work, a novel two-step acid leaching process was initiated for the synthesis of flocculants based on the reutilization of CGCS, and the acid leaching kinetics and flocculation mechanisms were investigated. The unique strategy of work lies in overcoming the limitation of acid leaching efficiency, improving the flocculation structure and performance. The following conclusions could be achieved.

(1) The optimum conditions for CGCS in HCl-acid leaching were as follows: concentration of 3.0 mol L<sup>-1</sup>, acid leaching temperature of 40 °C, acid leaching time of 1.5 h, and liquid–solid ratio of 15 : 1. The optimum conditions for CGCS in HAc-acid leaching were as follows: concentration of 5.0 mol L<sup>-1</sup>, acid leaching temperature of 40 °C, acid leaching time of 2.0 h, and liquid–solid ratio of 15 : 1. The optimum leaching of CGCS by HCl solution was 85.76%, and the optimum leaching of CGCS by HAc solution was 44.32%.

(2) The optimal preparation conditions of PAFAC were as follows: the volume ratio was 3 : 2, the polymerization pH was 3.5, the reaction temperature was 70 °C, and the reaction time was 3.0 h. Based on the XRF, XRD, FT-IR, and SEM characterization of PAFAC, it could be concluded that PAFAC was a kind of amorphous polymer containing Al, Fe, and Ca with a close gel network structure.

(3) PAFAC showed good performance in the treatment of domestic sewage, riverwater and aquaculture wastewater. Especially in the treatment of domestic sewage, PAFAC had excellent performance in the removal of turbidity, COD, and TP compared with that of flocculant A and B, which were only prepared by HCl and HAc, respectively.

(4) The acid leaching kinetics revealed that the acid leaching process of both acids coincided with both equations of the unreacted shrinkage core model and that both involved surface chemical reaction and loose layer diffusion. Moreover, the flocculation mechanisms demonstrated that charge neutralization, adsorption bridging dominated the flocculation process and precipitation net trapping played simultaneous roles in the flocculation.

The work has developed a new method for the safe disposal of CGCS and provides a novel way for the preparation of Fe–Al composite flocculants, especially, offering a potential strategy for the promotion of the additional value of the coal chemical industry. In addition, due to its good flocculation performance, PAFAC is expected to be a feasible pathway to treat coal gasification wastewater, coal chemical wastewater and mine wastewater associated with the activated sludge process.

## Author contributions

Haoqi Pan: writing – original draft, methodology, formal analysis; Tingting Shen, Jing Sun: writing – review & editing, conceptualization, funding acquisition, resources; Chenxu Sun, Haoqi Pan, Shaocang He, Tianpeng Li: formal analysis; Xuqian Lu: methodology.

## Conflicts of interest

The authors declare that they have no known competing financial interests or personal relationships that could have appeared to influence the work reported in this paper.

## Acknowledgements

The study was financially supported by the Foundation (No. ZZ20210124) of State Key Laboratory of Biobased Material and Green Papermaking, Qilu University of Technology, Shandong Academy of Sciences; National College Students' Innovation and Entrepreneurship Training Program (No. 202110431079), and Qilu University of Technology (Shandong Academy of Sciences) Basic Research Project of Science, Education and Industry Integration Pilot Project (No. 2022PY047).

## References

- 1 F. Guo, H. Wang, H. Li, S. Guo, Y. Guo, G. Qiu, H. Du, Y. Zhang, J. Wu and H. Zhang, *Fuel*, 2023, **339**, 126924.
- 2 X. Liu, Z. Jin, Y. Jing, P. Fan, Z. Qi, W. Bao, J. Wang, X. Yan, P. Lv and L. Dong, *Chin. J. Chem. Eng.*, 2021, **35**, 92–106.
- 3 J. Han, D. Jia, Q. Hui, L. Cui, Z. Zhu and C. Cao, *Geohazard Mech.*, 2023, S294974182300033X.
- 4 Z. Xue, C. Yang, L. Dong, W. Bao, J. Wang and P. Fan, *Sep. Purif. Technol.*, 2023, **304**, 122394.
- 5 W. Li, Z. Yu and G. Guan, *Carbon Resour. Convers.*, 2021, **4**, 89–99.
- 6 D. Wang, W. Meng, H. Zhou, Y. Yang, J. Xie, S. Yang and G. Li, *J. Cleaner Prod.*, 2022, **339**, 130500.
- 7 K. B. Kabir, K. Hein and S. Bhattacharya, *Comput. Chem. Eng.*, 2013, **48**, 96–104.
- 8 F. Guo, Y. Guo, Z. Guo, Z. Miao, X. Zhao, Y. Zhang, J. Li and J. Wu, *ACS Sustain. Chem. Eng.*, 2020, **8**, 8830–8839.
- 9 U. Arena, *Waste Manage.*, 2012, **32**, 625–639.
- 10 Z. Li, Y. Zhang, H. Zhao, H. Chen and R. He, *Constr. Build. Mater.*, 2019, **213**, 265–274.
- 11 A. G. Kim, *Fuel*, 2009, **88**, 1444–1452.
- 12 B. Lv, X. Deng, F. Jiao, B. Dong, C. Fang and B. Xing, *Process Saf. Environ. Prot.*, 2023, **171**, 859–873.
- 13 J. Xin, L. Liu, Q. Jiang, P. Yang, H. Qu and G. Xie, *Constr. Build. Mater.*, 2022, **322**, 125936.
- 14 A. Mohammadinia, A. Arulrajah, J. Sanjayan, M. M. Disfani, M. Win Bo and S. Darmawan, *J. Mater. Civ. Eng.*, 2016, **28**, 04016033.
- 15 T. Liu, S. K. Awasthi, Y. Duan, Z. Zhang and M. K. Awasthi, *Bioresour. Technol.*, 2020, **304**, 123024.
- 16 D. Zhu, S. Miao, B. Xue, Y. Jiang and C. Wei, *Water, Air, Soil Pollut.*, 2019, **230**, 155.
- 17 Y. Xiang, Y. Xiang, L. Wang and X. Li, *Environ. Sci. Pollut. Res.*, 2018, **25**, 11636–11645.
- 18 N. Yuan, K. Tan, X. Zhang, A. Zhao and R. Guo, *Chemosphere*, 2022, **303**, 134839.
- 19 X. Ma, Y. Li, D. Xu, H. Tian and H. Yang, *J. Environ. Manage.*, 2022, **305**, 114404.



- 20 Q. Qiao, H. Zhou, F. Guo, R. Shu, S. Liu, L. Xu, K. Dong and Y. Bai, *J. Cleaner Prod.*, 2022, **379**, 134739.
- 21 S. He, T. Li, T. Shen, J. Sun, H. Pan, C. Sun, W. Lu, X. Lu, G. Gao, Y. Fan, R. Li, E. Zhang and D. Yu, *Process Saf. Environ. Prot.*, 2023, **173**, 249–262.
- 22 W. Ai, Y. Li, X. Zhang, L. Xiao and X. Zhou, *Environ. Sci. Pollut. Res.*, 2022, **29**, 88894–88907.
- 23 C. Li, R. Liu, J. Zheng, L. Liao and Y. Zhang, *Int. J. Hydrogen Energy*, 2022, **47**, 12528–12538.
- 24 Z. Miao, J. Xu, L. Chen, R. Wang, Y. Zhang and J. Wu, *Fuel*, 2022, **309**, 122334.
- 25 C. S. Lee, M. F. Chong, J. Robinson and E. Binner, *Ind. Eng. Chem. Res.*, 2014, **53**, 18357–18369.
- 26 J. El-Gaayda, F. E. Titchou, R. Oukhrib, P.-S. Yap, T. Liu, M. Hamdani and R. Ait Akbour, *J. Environ. Chem. Eng.*, 2021, **9**, 106060.
- 27 G. Lu, T. Zhang, L. Ma, Y. Wang, W. Zhang, Z. Zhang and L. Wang, *Hydrometallurgy*, 2019, **188**, 248–255.
- 28 Y. Cheng, L. Xu and C. Liu, *Environ. Technol. Innovation*, 2022, **27**, 102509.
- 29 Y. Zhang, M. Li, D. Liu, X. Hou, J. Zou, X. Ma, F. Shang and Z. Wang, *Environ. Technol.*, 2019, **40**, 1568–1575.
- 30 J. Gao, B. Wang, W. Li, L. Cui, Y. Guo and F. Cheng, *Sep. Purif. Technol.*, 2023, **306**, 122545.
- 31 M. Brubaker, B. W. Stewart, R. C. Capo, K. T. Schroeder, E. C. Chapman, L. J. Spivak-Birndorf, D. J. Vesper, C. R. Cardone and P. C. Rohar, *Appl. Geochem.*, 2013, **32**, 184–194.
- 32 Y. Zhang, J. Sun, G. Lü, T. Zhang and Y. Gong, *Trans. Nonferrous Met. Soc. China*, 2023, **33**, 1932–1942.
- 33 Z. Zhao, R. Wang, J. Shu, M. Chen, Z. Xu, T. Xue, X. Zeng, D. He, D. Tan, Z. Deng and K. Ai, *Miner. Eng.*, 2022, **189**, 107862.
- 34 H. Islas, M. U. Flores, I. A. Reyes, J. C. Juárez, M. Reyes, A. M. Teja, E. G. Palacios, T. Pandiyan and J. Aguilar-Carrillo, *J. Hazard. Mater.*, 2020, **386**, 121664.
- 35 Y. Zheng and K. Chen, *Trans. Nonferrous Met. Soc. China*, 2014, **24**, 536–543.
- 36 J. Zhang, J. Zuo, Y. Jiang, D. Zhu, J. Zhang and C. Wei, *Solid State Sci.*, 2020, **100**, 106084.
- 37 Z. Lin, C. Zhang, C. Sun, W. Lu, B. Quan, P. Su, X. Li, T. Zhang, J. Guo and W. Li, *Sep. Purif. Technol.*, 2023, **327**, 124870.
- 38 H. Wang, Q. Zhang, J. Bian and D. Zhang, *Environ. Technol. Innovation*, 2023, **30**, 103096.
- 39 W. P. Cheng, *Chemosphere*, 2002, **47**, 963–969.
- 40 T.-K. Liu and E. S. K. Chian, *J. Colloid Interface Sci.*, 2005, **284**, 542–547.
- 41 L. Yan, Y. Wang, J. Li, H. Shen, C. Zhang and T. Qu, *Desalin. Water Treat.*, 2016, **57**, 18260–18274.
- 42 B. Liu, P. An, J. Chen, X. Xu, L. Liu and F. Yang, *Process Saf. Environ. Prot.*, 2020, **140**, 380–391.
- 43 A. I. Zouboulis, P. A. Moussas and F. Vasilakou, *J. Hazard. Mater.*, 2008, **155**, 459–468.
- 44 N. D. Tzoupanos, A. I. Zouboulis and C. A. Tsoleridis, *Colloids Surf., A*, 2009, **342**, 30–39.
- 45 Y. Zhang, S. Li, X. Wang, X. Ma, W. Wang and X. Li, *Sep. Purif. Technol.*, 2015, **146**, 311–316.
- 46 S. Yang, W. Li, H. Zhang, Y. Wen and Y. Ni, *Sep. Purif. Technol.*, 2019, **209**, 238–245.
- 47 Y. Liu, J. Ma, L. Lian, X. Wang, H. Zhang, W. Gao and D. Lou, *Process Saf. Environ. Prot.*, 2021, **155**, 287–294.
- 48 A. Hasan and P. Fatehi, *Sep. Purif. Technol.*, 2018, **207**, 213–221.
- 49 C. Ding, A. Xie, Z. Yan, X. Li, H. Zhang, N. Tang and X. Wang, *J. Water Process Eng.*, 2021, **40**, 101899.
- 50 Z. Lin, C. Zhang, Y. Hu, P. Su, B. Quan, X. Li and Z. Zhang, *J. Cleaner Prod.*, 2023, **399**, 136582.
- 51 Z. Ferasat, R. Panahi and B. Mokhtarani, *J. Environ. Manage.*, 2020, **255**, 109939.
- 52 R. Khiari, S. Dridi-Dhaouadi, C. Aguir and M. F. Mhenni, *J. Environ. Sci.*, 2010, **22**, 1539–1543.
- 53 K. Yang, G. Wang, X. Chen, X. Wang and F. Liu, *Colloids Surf., A*, 2018, **558**, 384–391.
- 54 Q. Teng, Z. Yang, B. Li, Z. Xie and S. Liu, *Colloids Surf., A*, 2023, **676**, 132250.
- 55 X. Huang, Y. Zhang, X. Li, J. Duan, B. Xu, S. Xia and P. Dong, *J. Water Process Eng.*, 2020, **36**, 101267.
- 56 L. Zhang, X. Liu, M. Zhang, T. Wang, H. Tang and Y. Jia, *J. Environ. Chem. Eng.*, 2023, **11**, 109312.
- 57 M. Han, Y. Dong, L. Dong, N. Guo and D. Wu, *J. Water Process Eng.*, 2023, **54**, 103952.
- 58 M. E. M. Ali, S. M. A. Moniem, B. A. Hemdan, N. S. Ammar and H. S. Ibrahim, *S. Afr. J. Chem. Eng.*, 2022, **42**, 127–137.
- 59 Y. Zeng and J. Park, *Colloids Surf., A*, 2009, **334**, 147–154.
- 60 X. Quan and H. Wang, *Chin. J. Chem. Eng.*, 2014, **22**, 1055–1060.
- 61 R. Subramanian, S. Zhu and R. H. Pelton, *Colloid Polym. Sci.*, 1999, **277**, 939–946.
- 62 L. D. Benefield, J. F. Judkins and B. L. Weand, *Process Chemistry for Water and Wastewater Treatment*, Prentice-Hall, Englewood Cliffs, N. J., 1982.
- 63 S. Sadri Moghaddam, M. R. Alavi Moghaddam and M. Arami, *J. Environ. Manage.*, 2011, **92**, 1284–1291.
- 64 J. Liu, Y. Zhu, Y. Tao, Y. Zhang, A. Li, T. Li, M. Sang and C. Zhang, *Biotechnol. Biofuels*, 2013, **6**, 98.
- 65 T. Chen, B. Gao and Q. Yue, *Colloids Surf., A*, 2010, **355**, 121–129.
- 66 G. Zhu, H. Zheng, W. Chen, W. Fan, P. Zhang and T. Tshukudu, *Desalination*, 2012, **285**, 315–323.
- 67 H. Zhao, H. Liu and J. Qu, *Colloids Surf., A*, 2011, **379**, 43–50.
- 68 U. A. Toor, H. Shin and D.-J. Kim, *J. Ind. Eng. Chem.*, 2019, **71**, 425–434.
- 69 T. U. Ali and D.-J. Kim, *Bioresour. Technol.*, 2016, **217**, 233–238.

